

Economic Dispatch of a Single Micro-Gas Turbine Under CHP Operation with Uncertain Demands

Miel Sharf, Iliya Romm, Michael Palman, Daniel Zelazo, and Beni Cukurel

Abstract—This work considers the economic dispatch problem for a single micro-gas turbine, governed by a discrete state-space model, under combined heat and power (CHP) operation and coupled with a utility. If the exact power and heat demands are given, existing algorithms can be used to give a quick optimal solution to the economic dispatch problem. However, in practice, the power and heat demands can not be known deterministically, but are rather predicted, resulting in an estimate and a bound on the estimation error. We consider the case in which the power and heat demands are unknown, and present a robust optimization-based approach for scheduling the turbine’s heat and power generation, in which the demand is assumed to be inside an uncertainty set. We consider two different choices of the uncertainty set relying on the ℓ^∞ - and the ℓ^1 -norms, each with different advantages, and consider the associated robust economic dispatch problems. We recast these as robust shortest-path problems on appropriately defined graphs. For the first choice, we provide an exact linear-time algorithm for the solution of the robust shortest-path problem, and for the second, we provide an exact quadratic-time algorithm and an approximate linear-time algorithm. The efficiency and usefulness of the algorithms are demonstrated using a detailed case study that employs real data on energy demand profiles and electricity tariffs.

I. INTRODUCTION

In recent years, the demand for energy has been ever-increasing [1]. Recent surveys and studies predict that electricity demand in 2050 will nearly double with respect to the its value in 2000 [2], [3]. Towards satisfying this ever-growing energy need, the choice of energy generation mechanism has serious economic consequences. On a global scale, a decrease in coal-based and nuclear-based generation is expected, and in fact, recent surveys predict that until 2050, most power will be supplied from renewable resources, as well as natural gas [2]. However, the production of renewable energy (and especially wind and solar energy) is highly dependent on the time of day, the season, the weather, and other natural phenomena beyond our control, meaning that re-dispatches by grid operators are essential. Thus, the renewables alone cannot control the future generation infrastructure. As a result, most developed countries have started to introduce natural gas turbines into the power grid, e.g. the power generation from natural gas in the European Union has tripled from the 1990s to the early 2000s [4].

M. Sharf (sharf@kth.se) is with the Division of Decision and Control Systems, KTH Royal Institute of Technology, Stockholm, Sweden. I. Romm (iliya@technion.ac.il), M. Palman (p.michael@technion.ac.il), D. Zelazo (dzelazo@technion.ac.il), and B. Cukurel (beni@cukurel.org) are with the Faculty of Aerospace Engineering, Technion - Israel Institute of Technology, Haifa, Israel.

This increase in the usage of natural gas is anticipated to further accelerate due to the introduction of combined cycle systems, where local consumers provide electricity, hot water and heat for themselves [4], [5]. The attractiveness of such combined heating and power (CHP) units was shown in recent studies [6], [7]. Micro gas- turbines (MGT) offer many advantages for small-scale CHP production, such as high power-to-weight ratio, low greenhouse gas emissions, reduced noise, theoretical high thermal efficiency and reliability. MGTs are agile and flexible due to their low mechanical and thermal inertia, meaning they are capable of short start-up times and rapid transitions between partial and full-load. For this reason, recent studies examined the economically favorable conditions toward integrating MGT powered CHP units into the smart-grid [8]–[11]. However, these works consider a generic MGT model and do not include realistic heat/power demand profiles or the variable pricing of electricity. More recently, accounting for realistic MGT performance modeling, consumer demand profiles and pricing, Ref. [12] presented a solution to the CHP economic dispatch (ED) problem for a single MGT coupled to the utility, i.e. an economically-optimal schedule of a MGT for a consumer generating its own power and heat.

Generally, ED considers a collection of supply mechanisms generating power and/or heat. The goal is to schedule the machines’ generation to guarantee that the demand is met, while minimizing the overall production costs [13]. ED has been considered for many different types of systems, including steam engines, gas turbines, and wind turbines [12], [14]–[20]. Most literature on ED simulate the generators as having continuous states based on first-principle modeling of the system, where the generated power and heat can take any value between a minimum and a maximum capacity, and that the corresponding cost function, mapping generation level to economic cost, is assumed to be quadratic [14], [16]. Classical solution approaches use techniques from convex optimization (e.g., gradient descent, the Lagrangian and duality) [15], [17], [21]. Some recent works couple these techniques with multi-agent theory and the consensus algorithm [16], [18]. Dynamic programming methods for this case also exist, but they suffer from the curse of dimensionality [22], [23], or that they guarantee only local optimality [24].

However, this convex optimization framework fails to capture some fundamental constraints in the problem unless augmented appropriately. First, in a low-demand scenario, not all providers should be active, so we should also schedule their startup and shutdown. This is usually done by considering the unit commitment problem [25]. However, due to the flexibility of MGTs and their quick start up and shutdown times, as

well as the fact that many MGTs can only shutdown from or startup to certain operation levels [26], [27], this decoupling will result in a wasteful scheduling policy. Therefore, we do not decouple the unit commitment and ED problems. The incorporation of the inactive state into ED is often considered by introducing binary variables which determine when the machines should be active [14], [15]. Second, when some MGTs are turned off, they must be cooled down before they could be turned on again, meaning that a single ‘off’ state is not enough to model the MGT. For example, the Capstone C65 MGT must cool down for up to 10 minutes before coming online again [26]. Lastly, even when the turbines are active, not any generation level between the maximum and minimum capacity is allowed. This is due to structural and rotordynamic resonances rendering the engines unstable or unsafe for certain rotation speeds [12], [19], [28]–[30].

Combining these restrictions, we get a model for the MGT having multiple discrete ‘off’ states and complex constraints on the allowed generation level when active, resulting in a constrained mixed-integer optimization problem. One possible solution is to discretize the state space and cost function, which works well for complex engine models, as the fuel consumption can be computed numerically. In this setting, the combined unit commitment and ED problems can be modeled as a discrete-time optimal control problem with a discrete state-space representation for the plant. This is an integer optimization problem where generated power and heat can only take values within a finite set. A solution to this problem is available using dynamic programming, namely by using the shortest-path algorithm on an appropriately defined graph [12], [31]. However, most approaches for ED assume that the demands are known throughout the time horizon [12], [15], [17], [20]–[23], e.g. by using one of the many load forecasting techniques that appear in the literature, [32]–[35] and references therein.

One might try to simply ignore the issue of unknown future demands by solving the ED problem with respect to an ad-hoc estimate of the demand level. However, this approach can fail miserably, as is known that for some real-world optimization problems, the optimal solution changes drastically when some parameters in the problem change even by a minuscule amount [36], [37]. Another approach to overcome this problem is to consider a stochastic optimization framework, in which we try and minimize the average cost of generation [38]–[40]. These require prior knowledge of the probability distribution of the underlying uncertainty, which must be estimated from past data, resulting again in the same problem of parameter inaccuracy. Another approach taken by recent studies is the incorporation of robust optimization techniques.

In robust optimization, one considers an optimization problem with uncertain parameters. These are assumed to be within a given set, known as the uncertainty set. The goal is to minimize a cost which considers all possible situations, most commonly the worst-case cost [36]. The uncertainty set is usually modeled from past data or engineering intuition. In [41]–[45], the robust optimization framework is used to handle uncertainty for wind generators and demand response. In [45], [46], this framework is used to handle demand uncertainty.

However, all of these assume that the turbines have continuous state-space models, and thus prohibit the considerations of cool-down period during shut down and unattainable operating conditions due to the mechanical resonances. To the best of the authors’ knowledge, the robust optimization framework has not been previously applied for the ED problem with a discrete state-space model. It should be noted that the robust economic dispatch problem in the continuous case is solvable using linear programming or second-order cone programming techniques, depending on the choice of the uncertainty set [41]–[43], whereas in the discrete case, one must rely on graph optimization algorithms, which are mixed-integer solvers.

Robust shortest-path problems are known to be generally NP-hard [47], meaning that a careful treatment of the problem and the uncertainty set is needed to assure that the resulting optimization problem is tractable. In [48], [49], the authors assume that the costs of the edges are independent of one another, and choose an uncertainty set consisting of confidence intervals for the cost without budgeting the uncertainty. Hence, the achieved solution is also robust against the case in which all edges incur the maximum possible cost, which is unrealistic in many scenarios. This issue is addressed in [50], in which a budgeted uncertainty set is considered by bounding the amount of edges whose cost can be different than the nominal value. This method cannot be applied to the problem of ED, as the costs of the edges are demand-dependent, and in practice, the demand will be different from our estimate at any time step, even if by a small amount. Moreover, all of these methods assume that the edge costs are uncorrelated with each other. However, in shortest-path problems inspired by economic dispatch, e.g. in [12], the costs of edges corresponding to the same time step are correlated, as both are determined by the demand at the corresponding time step. More recent works consider either a more complex uncertainty budgeting mechanism [51], or a more sophisticated robustification method [52]. However, the former can yield NP-hard problems [51], while the latter yields problems which take a long amount of time to solve in practice, even for small graphs with only hundreds of nodes [52]. For comparison, the MGT ED problem in [12] is converted to a shortest-path problem on a graph with roughly 250,000 nodes.

In this work, we consider the ED problem of a single MGT with a known discrete state-space representation, and unknown power and heat demands. The turbine is also connected to a utility from which power and heat can be purchased at a time-dependent cost¹. We apply the robust optimization framework for the mixed-integer ED problem. We study multiple possible choices for the uncertainty set, including a case in which the demand in each time is within a given confidence interval, and a case in which the uncertainty is budgeted throughout the time horizon. In both cases, we present linear-time algorithms for finding the optimal solution, and prove their validity. To the best of the authors’ knowledge, the algorithms we present are

¹Heat is not directly sold by the utility, but can be modeled as an additional fuel or electricity cost. Most consumers use a boiler to satisfy their heat demand, in which case one can model the heating cost with the price of natural gas.

the first to give a tractable solution to the robust shortest path problem in which the edge costs are correlated.

The rest of the paper is structured as follows. Section II presents the discrete state-space model for the turbine and the classical ED problem, as well as an interpretation of the problem as a shortest-path problem on an appropriate graph. It also briefly introduces the notion of robust optimization. Section III considers the robust ED problem as a worst-case shortest-path problem, including multiple possible cases for the uncertainty set, and presents efficient algorithms for solving the robust ED problem in these cases. Section IV portrays a case study demonstrating the algorithms.

Preliminaries: We use notions from graph theory [53]. A directed graph $\mathcal{G} = (\mathcal{V}, \mathcal{E})$ consists of a finite set of vertices \mathcal{V} and a set of edges \mathcal{E} which are pairs of vertices of \mathcal{V} . An edge from $u \in \mathcal{V}$ to $v \in \mathcal{V}$ will be denoted as $u \rightarrow v$, where u is the tail of the edge and v is its head. A path from a vertex u to a vertex v is a sequence of edges e_1, \dots, e_ℓ such that u is e_1 's tail, v is e_ℓ 's head, and for any i , e_i 's head is e_{i+1} 's tail. A directed graph \mathcal{G} is called a DAG (directed acyclic graph) if there are no paths which begin and end at the same vertex. For a node $v \in \mathcal{V}$, the in-degree $\deg(v)$ is the number of edges $e \in \mathcal{E}$ which have v as a head. As each edge has exactly one head, we have that $\sum_{v \in \mathcal{V}} \deg(v) = |\mathcal{E}|$. A weighted directed graph is a triplet $(\mathcal{V}, \mathcal{E}, w)$ where $(\mathcal{V}, \mathcal{E})$ is a directed graph and $w : \mathcal{E} \rightarrow \mathbb{R}$ is called the weight function. The cost of a path is defined as the sum of the weights of its edges. The shortest path problem for a graph \mathcal{G} is a combinatorial optimization problem in which the goal is to find the path with the smallest cost from a node s to a node q .

We also consider some notions from convex analysis [54]. For a convex set $\mathcal{W} \subset \mathbb{R}^d$, a point $x \in \mathcal{W}$ is called an *extreme point* if for any $y, z \in \mathcal{W}$ and any $t \in (0, 1)$, if $x = ty + (1 - t)z$ then $x = y = z$. The collection of extreme points of \mathcal{W} will be denoted by $\text{ext}(\mathcal{W})$. If $f : \mathcal{W} \rightarrow \mathbb{R}$ is a convex function and \mathcal{W} is bounded and closed, it is known that $\max_{x \in \mathcal{W}} f(x) = \max_{x \in \text{ext}(\mathcal{W})} f(x)$ [54, Theorem 32.2]. Given a norm $\|\cdot\|$ on \mathbb{R}^N , the norm ball of radius $r > 0$ around a point $x_0 \in \mathbb{R}^N$ is given by the set $\{x \in \mathbb{R}^N : \|x - x_0\| \leq r\}$. Moreover, a weighted ℓ^∞ norm on \mathbb{R}^N is given by $\|x\| = \max_{i=1}^N \{w_i |x_i|\}$ where $w_1, \dots, w_N > 0$ are the associated weights. Similarly, a weighted ℓ^1 -norm is given by $\|x\| = \sum_{i=1}^N w_i |x_i|$. The Minkowski sum of two sets A, B is given by $A + B = \{a + b : a \in A, b \in B\}$.

II. BACKGROUND

This section provides the required background material, including a model for the MGT, the ED problem and its relation to the shortest-path problem, and some basic notions from robust optimization.

A. Discrete State-Space Models for Turbines

We consider a micro-gas turbine (MGT) with a discrete state space, which is a generalization of [12]. We denote the state space of the MGT by \mathcal{X} . The state $x(t)$ of the turbine evolves in discrete time. The dynamics can be modeled by two functions f, c and a state-indexed set $\mathcal{U}(x)$. Namely, for

each $x \in \mathcal{X}$, we denote the set of admissible control signals by $\mathcal{U}(x)$, and consider the following state evolution:

$$x(t + c(x(t), u(t))\Delta t) = f(x(t), u(t)),$$

where $u(t)$ is the control input at time t and Δt is the time increment. The function $f(x, u)$ defines the allowable transitions between turbine states. The function $c(x, u)$ defines the transition times between states, and is assumed to take positive integer values. In other words, if the control input $u(t)$ is applied at the state $x(t)$, the next state will be $f(x(t), u(t))$ and it will take $c(x(t), u(t))\Delta t$ time to get there. For each state x and control input u , we let $P(x, u)$ be the power generation associated with the state-control pair (x, u) for one time step Δt , and let $H(x, u)$ be the heat generation associated with the same state-control pair for one time step Δt . For example, if x is an ‘off’ state and u is a control input such that $f(x, u)$ is also an ‘off’ state, then $P(x, u) = H(x, u) = 0$. We emphasize that both the power and heat generation can also depend on u . Indeed, because P, H aggregate the generation between two times t_0 and $t_0 + \Delta t$, the control $u(t_0)$ does not only determine the state of the turbine at time $t_0 + \Delta t$, but also the generated amount in the intermediate time, as even though our model is discrete-time, the turbine generates power in continuous-time.

Example 1. Consider the MGT model in [12], consisting of a single stage centrifugal compressor, a can-type combustor, a single stage turbine, a recuperator and a separate heat recovery unit. There, the active states of the turbine are characterized by two parameters, p and h . The variable p is the speed of the engine, and can take values p_1, \dots, p_s , while the variable h is the position of a recuperator bypass valve, and can take values h_1, \dots, h_v . The allowable transitions change the speed of the engine, the recuperator bypass valve position, or both by one level. Changing the position of the valve or slowing down the engine takes one unit of time, while revving up the engine takes two units of time.

Example 2. Consider a turbine that generates p units of power and h units of heat when active. When the turbine is on, it can be turned off at any time, within 15 seconds. However, once it is turned off, it has a cool-down time of 45 seconds (i.e., three time units). This turbine can be modeled using a discrete state-space representation with time instances $\Delta t = 20$ sec apart, and with $|\mathcal{X}| = 4$ possible states - one active state, x_{on} , and three off states, $x_{\text{off},1}, x_{\text{off},2}, x_{\text{off},3+}$, which represent that the turbine has been inactive for 1, 2, or at least 3 units of time, respectively. Here, $\mathcal{U}(x_{\text{on}}) = \{\text{keep}, \text{shutdown}\}$, $\mathcal{U}(x_{\text{off},3+}) = \{\text{keep}, \text{start}\}$, and $\mathcal{U}(x_{\text{off},1}) = \mathcal{U}(x_{\text{off},2}) = \{\text{keep}\}$. The control signal ‘keep’ moves x_{on} to itself, $x_{\text{off},1}$ to $x_{\text{off},2}$, $x_{\text{off},2}$ to $x_{\text{off},3+}$ and $x_{\text{off},3+}$ to itself. Moreover, the control signal ‘shutdown’ moves x_{on} to $x_{\text{off},1}$, and the control signal ‘start’ moves $x_{\text{off},3+}$ to x_{on} . These transitions all take one time step. The possible evolution of the state $x(t)$ of the turbine across 5 time steps can be seen in Fig. 1.

B. Economic Dispatch and the Shortest-Path Problem

The ED problem aims at scheduling the generation of the turbine throughout a time horizon T to minimize the cost while

generating the required amount of heat and power. For each state-control pair (x, u) , we define $C_T(x, u)$ as the total cost of operating the turbine for $c(x, u)$ units of time, starting at state x and issuing the control input u . In other words, this is the cost of the transition defined by the state-control pair (x, u) . We let $(P(t), H(t))_{t=1}^T$ be the power and heat demand, which are known throughout the time horizon.

Besides the turbine, we can also draw power and heat from a utility. For a time t , we denote the power and heat purchased from the utility by $x_U^P(t)$ and $x_U^H(t)$ respectively. The cost of purchasing x_U^P units of power and x_U^H units of heat from the utility at time t will be denoted by $C_{U,t}^P(x_U^P), C_{U,t}^H(x_U^H)$ respectively.

Both cost functions are assumed to be non-decreasing and defined for $x_U^P, x_U^H < 0$. For example, a negative cost corresponds to selling power to the utility, a zero cost corresponds to exhausting excess heat, and an infinite cost corresponds to inability to sell power/heat. The ED problem is the following optimization problem:

$$\begin{aligned} \min \quad & \sum_{t=1}^T \left[C_T(x(t), u(t)) + C_{U,t}^P(x_U^P(t)) + C_{U,t}^H(x_U^H(t)) \right] \quad (1) \\ \text{s.t.} \quad & x(t + c(x(t), u(t))\Delta t) = f(x(t), u(t)), \forall t = 1, \dots, T \\ & P(x(t), u(t)) + x_U^P(t) = P(t), \forall t \\ & H(x(t), u(t)) + x_U^H(t) = H(t), \forall t \\ & x(t) \in \mathcal{X}, \quad u(t) \in \mathcal{U}(x(t)), \quad x_U^P(t), x_U^H(t) \in \mathbb{R}, \forall t \end{aligned}$$

This problem is evidently a nonlinear mixed-integer problem. However, [12] offers a quick solution method. We build a directed graph $\mathcal{G} = (\mathcal{V}, \mathcal{E})$. The vertices are given by the pairs (t, x) where $t \in \{1, \dots, T\}$ and $x \in \mathcal{X}$. For a fixed time t , the nodes $\{(t, x)\}_{x \in \mathcal{X}}$ designate the state of the turbine at time t . As for the edges, $e = (t_1, x_1) \rightarrow (t_2, x_2) \in \mathcal{E}$ if there is some $u_1 \in \mathcal{U}(x_1)$ such that $f(x_1, u_1) = x_2$ and $t_2 = t_1 + c(x_1, u_1)$. The cost of said edge is defined as the total cost of the transition, given by the following expression:

$$w_e = C_T(x_1, u_1) + \sum_{t=t_1}^{t_2} [C_{U,t}^P(P(t) - P(x_1, u_1)) \quad (2) \\ + C_{U,t}^H(H(t) - H(x_1, u_1))].$$

The edges and their cost represent the possible transitions for the turbine. For example, the corresponding graph for the turbine in Example 2 with time horizon $T = 5$ can be seen in Fig. 1. Thus, a possible trajectory $(x(t))_{t=1}^T$ of the state of the turbine corresponds to a *path* in the graph². If we define the cost of a path as the sum of the costs of the corresponding edges, we get a one-to-one correspondence between paths on the graph \mathcal{G} and generation schedules of the turbine, in which the total cost of a schedule is identical to the cost of the corresponding path. Therefore, the ED problem for the MGT can be restated as finding the cheapest path from some node $(1, x)$ to some other node (T, y) , where $x, y \in \mathcal{X}$ are the initial and final state of the turbine.

Suppose we add a node s (called the source node) and a node q (called the terminal node) to the graph, and add edges $s \rightarrow (1, x)$, $(T, x) \rightarrow q$ from all $x \in \mathcal{X}$ having zero

²See the notations section for a precise definition of a path in a graph.

weight. Any path from some node $(1, x)$ to some other node (T, y) , where $x, y \in \mathcal{X}$, uniquely defines a path from s to q . Moreover, these path share the same cost. Thus, the ED problem can be understood as finding the cheapest path from s to q . This problem is known as the *shortest path problem* [31]. If we denote the set of all paths from s to q in \mathcal{G} by $\text{PATH}_{s \rightarrow q}(\mathcal{G})$, we get the following optimization problem in the variable $\text{Path}_{s \rightarrow q}$:

$$\begin{aligned} \min_{\text{Path}_{s \rightarrow q}} \quad & \sum_{e \in \text{Path}_{s \rightarrow q}} w_e \quad (3) \\ \text{s.t.} \quad & \text{Path}_{s \rightarrow q} \in \text{PATH}_{s \rightarrow q}(\mathcal{G}). \end{aligned}$$

As \mathcal{G} is a DAG, standard dynamic programming methods solve this problem quickly, with computational complexity equal to $O(|\mathcal{E}|)$. Moreover, standard graph theory software provides implementation of said methods. Thus, the ED problem for an MGT can be solved quickly using standard software.

However, this approach cannot be used when the heat and power demands are unknown and the weights of the edges cannot be determined accurately. Most of the time, an estimate on the demand throughout the horizon is known, so it is tempting to try and solve this problem with the estimate, disregarding the estimation error. However, the optimal solution to many complex real-life optimization problems can perform poorly when the parameters of the problems are changed by even a minuscule amount. [36], [37]. This motivates using tools from robust optimization, giving a bound on the worst-case behavior of a proposed solution.

C. Robust Optimization

Consider a minimization problem in the variable x , where both the cost function $F(x, \xi)$ and constraints $\phi(x, \xi) \leq 0$ are affected by an uncertain variable $\xi \in \Xi$, where the inequalities are understood component-wise. In our case, the uncertain

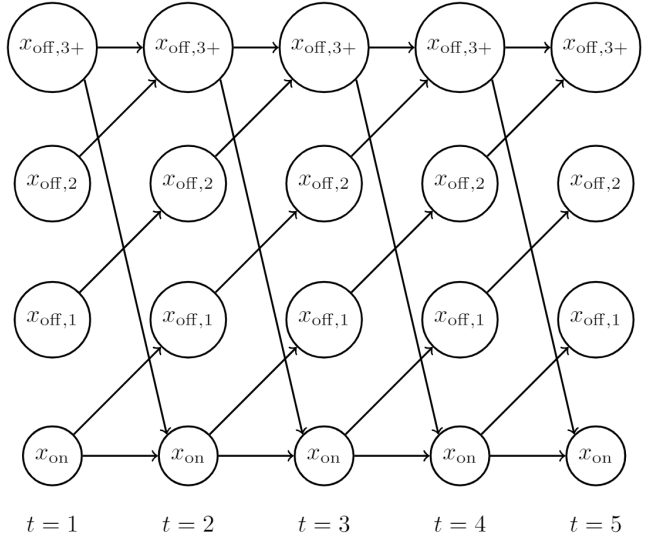


Fig. 1: The state transition graph corresponding to the ED problem for the turbine in Example 2 with time horizon $T = 5$.

variables are the power and heat demands. In classical robust optimization, we choose a subset $\mathcal{W} \subseteq \Xi$ defining all possible values of the uncertainty we consider, coined the *uncertainty set*, and define the worst-case optimization problem [36]:

$$\begin{aligned} \min_x \quad & \max_{\xi \in \mathcal{W}} F(x, \xi) \\ \text{s.t.} \quad & \phi(x, \xi) \leq 0, \quad \forall \xi \in \mathcal{W}. \end{aligned}$$

This optimization problem assures that the solution is feasible for any value of the uncertainty within the uncertainty set, and gives a bound on its cost. However, checking that $\phi(x, \xi) \leq 0$ for any $\xi \in \mathcal{W}$ is usually very hard or even impossible if \mathcal{W} is infinite. Instead, we reformulate the constraint as $\sup_{\xi \in \mathcal{W}} \phi(x, \xi) \leq 0$, which is easier to verify if the supremum can be computed analytically. For example, if ϕ is a bilinear function and \mathcal{W} is defined using finitely many linear inequalities, the constraint can be reformulated to be linear. A common choice for \mathcal{W} is $\mathcal{W} = \{\xi : \|\xi\| \leq \delta\}$, for which the supremum can be computed using the dual norm [36]. Common choices for $\|\cdot\|$ are the p -norm for some $p \in \{1, 2, \infty\}$. The parameter δ must be tuned accordingly to avoid over-conservatism as well as being too optimistic. See [55] for more on the implications of choosing a specific uncertainty set.

III. ROBUST ECONOMIC DISPATCH WITH UNCERTAIN DEMANDS

Consider an ED problem of the form (1), where the demand $\xi = (P(t), H(t))_{t=1}^T$ is assumed to be unknown. Assume further that the true demand profile is contained in a set $\mathcal{W} \subseteq \mathbb{R}^{2T}$. Note that in the ED problem, the turbine variables $x(t), u(t)$ must be scheduled in advance, after which the true demand is revealed and the utility variables $x_U^P(t), x_U^H(t)$ are computed from the power- and heat-balance equations, $x_U^P(t) = P(t) - P(x(t))$ and $x_U^H(t) = H(t) - H(x(t))$. We use the graph-based interpretation of the problem. For every edge $e \in \mathcal{E}$, we let $w_e(\xi)$ be equal to (2), where $\xi = (P(t), H(t))_{t=1}^T$.

$$\begin{aligned} \min_{\text{Path}_{s \rightarrow q}} \quad & \max_{\xi \in \mathcal{W}} \sum_{e \in \text{Path}_{s \rightarrow q}} w_e(\xi) \\ \text{s.t.} \quad & \text{Path}_{s \rightarrow q} \in \text{PATH}_{s \rightarrow q}(\mathcal{G}). \end{aligned} \quad (\text{RSPP})$$

The main focus of this section is to study the tractability of (RSPP) as a consequence of the choice of \mathcal{W} .

A. Positively-Extreme Profiles and \mathcal{L}_∞ -based Uncertainty

The tractability of (RSPP) boils down to the following question - what demand profiles ξ are the worst-case for a specific path in the graph \mathcal{G} ? Intuitively, the higher the demand, the higher the generation cost. It is easy to see by (2) that if $P_1(t) \leq P_2(t)$ and $H_1(t) \leq H_2(t)$ for all t , then $w_e(\xi_1) \leq w_e(\xi_2)$ for every $e \in \mathcal{E}$, where $\xi_i = (P_i(t), H_i(t))_{t=1}^T$ for $i = 1, 2$. Thus, for any $\xi_1, \xi_2 \in \mathbb{R}^{2T}$, we have:

$$(\xi_1)_k \leq (\xi_2)_k, \quad \forall k = 1, \dots, 2T \implies w_e(\xi_1) \leq w_e(\xi_2). \quad (4)$$

This suggests the following definition:

Definition 1. Let $\mathcal{W} \subseteq \mathbb{R}^{2T}$ be any set. We say that $\xi \in \mathcal{W}$ is *positively extreme* if for all $\zeta \in \mathcal{W}$ there exists some i such that $\xi_i > \zeta_i$. In other words, we cannot find a point in \mathcal{W} whose entries are all bigger than ξ 's. The collection of all positively extreme points in \mathcal{W} will be denoted as $\text{pe}(\mathcal{W})$.

Example 3. If $\mathcal{W} = \{\xi \in \mathbb{R}^{2T} : \max_i a_i |\xi_i| \leq \mu\}$ then $\text{pe}(\mathcal{W})$ contains only the point $(\frac{\mu}{a_1}, \dots, \frac{\mu}{a_{2T}})$.

Example 4. If $\mathcal{W} = \{\xi \in \mathbb{R}^{2T} : \sum_i a_i |\xi_i| \leq \mu\}$, $\text{pe}(\mathcal{W})$ contains all points ξ such that $\xi_i \geq 0$ and $\sum_i a_i \xi_i = \mu$. In particular, $\text{pe}(\mathcal{W})$ is infinite.

Theorem 1. Let \mathcal{W} be any bounded closed subset of \mathbb{R}^{2T} , and assume all functions w_e satisfy (4). The problem (RSPP) for \mathcal{W} is equivalent to the problem (RSPP) for $\text{pe}(\mathcal{W})$, i.e.,

$$\min_{\text{Path}_{s \rightarrow q}} \max_{\xi \in \mathcal{W}} \sum_{e \in \text{Path}_{s \rightarrow q}} w_e(\xi) = \min_{\text{Path}_{s \rightarrow q}} \max_{\xi \in \text{pe}(\mathcal{W})} \sum_{e \in \text{Path}_{s \rightarrow q}} w_e(\xi). \quad (5)$$

Proof. Take any path $\text{Path}_{s \rightarrow q}$ from s to q , and let e_1, \dots, e_ℓ be its edges. We show that $\max_{\xi \in \mathcal{W}} \sum_{i=1}^\ell w_{e_i}(\xi) = \max_{\xi \in \text{pe}(\mathcal{W})} \sum_{i=1}^\ell w_{e_i}(\xi)$. Take some $\zeta \in \mathcal{W}$. We claim that there exists a point $\xi \in \text{pe}(\mathcal{W})$ such that $\zeta_i \leq \xi_i$ for all i . Indeed, this is true because the set $\mathcal{W} \cap \{\xi : \zeta_i \geq \xi_i\}$ is also bounded and closed, hence it has a positively-extreme point, which must be in $\text{pe}(\mathcal{W})$ by definition. In particular, we conclude by (4) that

$$\sum_{i=1}^\ell w_{e_i}(\zeta) \leq \sum_{i=1}^\ell w_{e_i}(\xi) \leq \max_{\xi \in \text{pe}(\mathcal{W})} \sum_{i=1}^\ell w_{e_i}(\xi).$$

Maximizing over $\zeta \in \mathcal{W}$ completes the proof. \square

We now examine a corollary of Theorem 1 that considers an estimate for the power and heat demand at a time t , denoted by $P_0(t), H_0(t)$ respectively, and an estimation error that is bounded by variables $\Delta P(t), \Delta H(t)$ respectively.

Corollary 1. Suppose that the set \mathcal{W} is given by:

$$\mathcal{W} = \left\{ (P(t), H(t))_{t=1}^T : \begin{array}{l} |P(t) - P_0(t)| \leq \Delta P(t), \\ |H(t) - H_0(t)| \leq \Delta H(t) \end{array} \right\}, \quad (6)$$

The robust ED problem with uncertainty set \mathcal{W} is equivalent to the ED problem with demand $P(t) = P_0(t) + \Delta P(t)$, $H(t) = H_0(t) + \Delta H(t)$. Thus, it can be solved in $O(|\mathcal{E}|) = O(\max_{x, u} c(x, u) |\mathcal{X}| |\mathcal{T}|)$ time.

Proof. It's enough to show that (RSPP) for the set \mathcal{W} is equivalent to the shortest path problem with weights $w_e(\xi)$ for $\xi = (P_0(t) + \Delta P(t), H_0(t) + \Delta H(t))_{t=1}^T$. This follows immediately from Theorem 1 and the fact that by definition, $\text{pe}(\mathcal{W}) = (P_0(t) + \Delta P(t), H_0(t) + \Delta H(t))_{t=1}^T$. The time complexity $O(|\mathcal{E}|)$ is the time it takes to find the shortest path in a directed acyclic graph [31]. \square

The corollary above shows that the robust ED problem can be solved in a tractable manner if \mathcal{W} has the form (6), as it is equivalent to a shortest-path problem. However, in (6), the demand is merely assumed to be within given confidence intervals for each time step. This assumption might lead to mediocre results in practice - if the confidence intervals are taken too large, the solution may be over-conservative, and

if they are taken too small, we do not account for unforeseen short demand spikes. A common way to deal with this problem is to use uncertainty sets which also specify the 1-norm, i.e. they budget the uncertainty over all time steps. This will be the focus of the next subsection.

Before moving forward, we want to return to Example 4. There, $\text{pe}(\mathcal{W})$ was infinite, meaning that the problem $\max_{\xi \in \text{pe}(\mathcal{W})} \sum w_e(\xi)$ is hard to solve, unless more assumptions are added. If we assume the functions w_e are convex in ξ , the maximized function is also convex, so the maximum is attained at an extreme point of the set $\text{pe}(\mathcal{W})$ [54, Theorem 32.2]. It's easy to see that w_e is convex if and only if $C_{U,t}^P, C_{U,t}^H$ are convex functions for every time t .

Assumption 1. For every time t , the utility cost functions $C_{U,t}^P, C_{U,t}^H$ are convex. Equivalently, the cost functions w_e are convex.

Remark 1. The convexity of $C_{U,t}^P$ can be easily deduced for many cases. For example, the cost function implemented in European electricity markets is a linear function, in which the per-unit price is achieved by an optimization problem aggregating all the demands and generations in the network [56], [57]. If we assume that the demands $P(t), H(t)$ and the turbine generation are small enough to have a negligible effect on the per-unit cost, then $C_{U,t}^P$ is linear. In fact, even without this assumption, a larger demand would correspond to a higher per-unit cost, meaning that the cost function $C_{U,t}^P$ is convex. In other cases, service operators explicitly convexify this cost function [58].

Alternatively, utility operators put a fixed per-unit cost, as well as fixed costs and demand charges which only go into effect if the demand is positive [59]. In this case, if we cannot sell power back to the utility, then the achieved cost function is given by

$$C_{U,t}^P(x_U^P) = \begin{cases} A_t x_U^P + B_t, & x_U^P \geq 0 \\ \infty, & x_U^P < 0 \end{cases}$$

for some possibly time-dependent parameters A_t, B_t , meaning it is convex. If we instead consider the case in which there is only a fixed per-unit cost and a fixed cost, then $C_{U,t}^P$ is affine and thus convex.

For heat, most consumers use a boiler to satisfy their heat demand, in which case one can model the heating cost with the price of natural gas. In that case, the cost function $C_{U,t}^H$ is given by

$$C_{U,t}^H(x_U^H) = \begin{cases} A x_U^H, & x_U^H \geq 0 \\ 0, & x_U^H \leq 0 \end{cases}$$

as excess heat can be exhausted with no extra cost. In particular, $C_{U,t}^H$ is convex. See [12] for more details.

In any case, if either of the functions $C_{U,t}^P, C_{U,t}^H$ is not convex, and Assumption 1 is needed, we approximate them by convex functions. This will result in a suboptimal solution for (RSPP), whose quality is closely related to the approximation error of $C_{U,t}^P, C_{U,t}^H$.

Under Assumption 1, we can prove an analogue of Theorem 1 which relies on the notion of extreme points:

Corollary 2. Let $\mathcal{W} \subseteq \mathbb{R}^2$ be bounded and closed, and assume w_e satisfies (4) and Assumption 1. The problem (RSPP) for \mathcal{W} is equivalent to the problem (RSPP) for $\text{ext}(\text{pe}(\mathcal{W}))$.

Proof. Fix any path $\text{Path}_{s \rightarrow q}$ from s to q , and let e_1, \dots, e_ℓ be its edges. We show that $\max_{\xi \in \mathcal{W}} \sum_{i=1}^\ell w_{e_i}(\xi) = \max_{\xi \in \text{ext}(\text{pe}(\mathcal{W}))} \sum_{i=1}^\ell w_{e_i}(\xi)$. First, by Theorem 1, we have that $\max_{\xi \in \mathcal{W}} \sum_{i=1}^\ell w_{e_i}(\xi) = \max_{\xi \in \text{pe}(\mathcal{W})} \sum_{i=1}^\ell w_{e_i}(\xi)$. Second, we note that $\sum_{i=1}^\ell w_{e_i}(\xi)$ is a convex function in ξ , so by [54, Theorem 32.2], for any closed bounded set \mathcal{A} we have that

$$\max_{\xi \in \mathcal{A}} \sum_{i=1}^\ell w_{e_i}(\xi) = \max_{\xi \in \text{ext}(\mathcal{A})} \sum_{i=1}^\ell w_{e_i}(\xi).$$

Choosing $\mathcal{A} = \text{pe}(\mathcal{W})$ completes the proof. \square

Example 5. If $\mathcal{W} = \{\xi \in \mathbb{R}^{2T} : \sum_i a_i |\xi_i| \leq \mu\}$, $\text{ext}(\text{pe}(\mathcal{W}))$ contains the $2T$ points $\xi^{(1)}, \dots, \xi^{(2T)}$, where $\xi_i^{(j)} = \frac{\mu}{a_i} \mathbf{1}_{\{i=j\}}$.

B. Mixed $\mathcal{L}_1 \setminus \mathcal{L}_\infty$ Uncertainty

For this subsection, we assume Assumption 1 holds. We want to consider an uncertainty set \mathcal{W} including both unforeseen short demand spikes as well as a constant bias from the estimate. A natural choice here is:

$$\mathcal{W} = \left\{ (P(t), H(t))_{t=1}^T : \begin{array}{l} |P(t) - P_0(t)| \leq \Delta P(t), \\ |H(t) - H_0(t)| \leq \Delta H(t) \\ \sum_{t=1}^T \left[\frac{|P(t) - P_0(t)|}{\Delta P(t)} + \frac{|H(t) - H_0(t)|}{\Delta H(t)} \right] \leq \mu \end{array} \right\}.$$

However, it is possible to show that unless $\frac{\mu}{2T} \ll 1$ or $1 - \frac{\mu}{2T} \ll 1$, $|\text{ext}(\text{pe}(\mathcal{W}))|$ is exponential in T . Thus, Corollary 2 will not yield a tractable optimization problem. Instead, we consider a different uncertainty set:

$$\mathcal{W} = \left\{ (P(t), H(t))_{t=1}^T : \begin{array}{l} P(t) = P_0(t) + \eta_1^P(t) + \eta_\infty^P(t), \\ H(t) = H_0(t) + \eta_1^H(t) + \eta_\infty^H(t), \\ \sum_{t=1}^T [|\delta_{P,t} \eta_1^P(t)| + |\delta_{H,t} \eta_1^H(t)|] \leq \mu_1, \\ |\eta_\infty^P(t)| \leq \Delta P(t), |\eta_\infty^H(t)| \leq \Delta H(t), \forall t \end{array} \right\}, \quad (7)$$

where $\mu_1, \Delta P(t), \Delta H(t), \delta_{P,t}, \delta_{H,t} \geq 0$ are parameters. This uncertainty set will be called the “mixed $\mathcal{L}_1/\mathcal{L}_\infty$ uncertainty set.” Intuitively, it dissects the uncertainty in the demand into two factors - the first, $\eta_1^P(t), \eta_1^H(t)$, corresponds to large-but-short unforeseen demand spikes, and the second, $\eta_\infty^P(t), \eta_\infty^H(t)$, corresponds to a small-but-long bias from the estimated demand, $(P_0(t), H_0(t))_{t=1}^T$. If $\mu_1, \Delta P(t), \Delta H(t), \delta_{P,t}, \delta_{H,t}$ are tuned correctly, the uncertainty set can model both without being too conservative. Similarly to Example 4, the set $\text{ext}(\text{pe}(\mathcal{U}))$ consists of $2T$ elements, $(\bar{P}(t) + \Delta P^{(i)}(t), \bar{H}_0(t))_{t=1}^T$ and $(\bar{P}_0(t), \bar{H}_0(t) + \Delta H^{(i)}(t))_{t=1}^T$ for $i = 1, \dots, T$, where:

$$\bar{P}_0(t) = P_0(t) + \Delta P(t), \quad \bar{H}_0(t) = H_0(t) + \Delta H(t). \quad (8)$$

$$\Delta P^{(i)}(t) = \frac{\mu_1}{\delta_{P,t}} \mathbf{1}_{\{i=t\}}, \quad \Delta H^{(i)}(t) = \frac{\mu_1}{\delta_{H,t}} \mathbf{1}_{\{i=t\}}.$$

The demands $\bar{P}_0(t)$ and $H_0(t)$ serve as a worst-case scenario if there are no demand spikes, similarly to Corollary 1. For each $i = 1, 2, \dots, T$, the terms $\Delta P^{(i)}, \Delta H^{(i)}$ correspond to the highest possible demand spike at time i . In particular, for any i ,

the sum of these terms serves as a possible worst-case scenario for the uncertainty set (7). Thus, the robust ED problem for \mathcal{W} is reduced to (RSPP) with $2T$ possible demand profiles - 2 demand profiles for each time i , in which the power or heat demand spikes at time i , respectively. We want to use an augmented form of the shortest-path algorithm to solve this problem. In order to do so, we first reformulate it as a problem closer to the classical shortest-path problem.

For each edge $e = (t_1, x_1) \rightarrow (t_2, x_2) \in \mathcal{E}$, we consider the cost w_e for all $2T$ possible scenarios. We first define $W_{\text{bias}}(e)$ as $w_e((\bar{P}_0(t), \bar{H}_0(t)))$, which is the cost on the edge e corresponding the worst-case spikeless demand, stemming only from the long-but-small bias in demand, which must be paid for each of the extreme $2T$ scenarios, no matter when the spike occurs. We also let $W_{\text{spike}}(e)$ be the highest possible additional cost stemming from unforeseen demand spikes, defined as

$$\begin{aligned} \max_{t_1 \leq k < t_2} \{w_e((\bar{P}_0(t) + \Delta P^{(k)}(t), \bar{H}_0(t))), \\ w_e((\bar{P}_0(t), \bar{H}_0(t) + \Delta H^{(k)}(t)))\} - W_{\text{bias}}(e), \end{aligned} \quad (9)$$

That is, $W_{\text{spike}}(e)$ is defined as the maximum possible cost of the edge e in any of the $2T$ possible scenarios, minus $W_{\text{bias}}(e)$. Given a path $\text{Path}_{s \rightarrow q}$ from s to q , the cost function $\max_{\xi \in \mathcal{W}} \sum_{e \in \text{Path}_{s \rightarrow q}} w_e(\xi)$ is the sum of $\sum_{e \in \text{Path}_{s \rightarrow q}} W_{\text{bias}}(e)$ and $\max_{e \in \text{Path}_{s \rightarrow q}} W_{\text{spike}}(e)$. Indeed, if the demand profile is equal to $(\bar{P}_0(t) + \Delta P^{(k)}(t), \bar{H}_0(t))_{t=1}^T$ or to $(\bar{P}_0(t), \bar{H}_0(t) + \Delta H^{(k)}(t))_{t=1}^T$, meaning there is a spike in demand at time k , then all edges corresponding to transitions outside time k only have the “bias” cost, while the single edge corresponding to a transition at time k has a $W_{\text{bias}} + W_{\text{spike}}$. Moreover, given any edge $e = (t_1, x_1) \rightarrow (t_2, x_2) \in \mathcal{E}$, there is at least one k for which this edge has an additional cost equal to W_{spike} . Thus, the optimization problem becomes:

$$\begin{aligned} \min \sum_{e \in \text{Path}_{s \rightarrow q}} W_{\text{bias}}(e) + \max_{e \in \text{Path}_{s \rightarrow q}} W_{\text{spike}}(e) \quad (10) \\ \text{s.t. } \text{Path}_{s \rightarrow q} \in \text{PATH}_{s \rightarrow q}(\mathcal{G}). \end{aligned}$$

We would like to consider an algorithm for solving the problem (RSPP) in this case. A key idea that will be used is to consider the graph \mathcal{G} with a different set of weights. For each number $\alpha \in \mathbb{R}$, we define the α -restricted graph \mathcal{G}_α as a weighted graph $(\mathcal{V}, \mathcal{E}, \omega_\alpha)$, where $\mathcal{G} = (\mathcal{V}, \mathcal{E})$ and $\omega_\alpha(e) = \begin{cases} W_{\text{bias}}(e) & W_{\text{spike}}(e) \leq \alpha \\ \infty & W_{\text{spike}}(e) > \alpha. \end{cases}$

We present the following algorithm for solving the problem. First, we compute all parameters as in (8), and define $W_{\text{bias}}, W_{\text{spike}}$ as above. Second, we define an array of thresholds called Thresh. For each threshold $\alpha \in \text{Thresh}$, we solve the classical shortest-path problem on the weighted graph \mathcal{G}_α . We let $V_{\text{path}}(\alpha)$ be this shortest path on \mathcal{G}_α , and let $V_{\text{cost}}(\alpha)$ as the total cost of this path in the problem (10). We then choose the return the path $V_{\text{path}}(\alpha)$ for which $V_{\text{cost}}(\alpha)$ is minimal over all thresholds α . We show that choosing the set of thresholds as $\{W_{\text{spike}}(e)\}_{e \in \mathcal{E}}$ guarantees that we achieve an optimal solution of (10).

Theorem 2. *Algorithm 1 solves (RSPP) for the uncertainty set \mathcal{W} of the form (7). Moreover, its computational complexity is $O(|\mathcal{E}|^2)$.*

Algorithm 1 Optimal Economic Dispatch for Mixed $\mathcal{L}_1/\mathcal{L}_\infty$ Uncertainty

Input: An uncertainty set \mathcal{W} of the form (7).

Output: An optimal solution to the corresponding robust economic dispatch problem.

- 1: Define $\bar{P}_0(t), \bar{H}_0(t), \Delta P^{(i)}(t), \Delta H^{(i)}(t)$ as in (8).
- 2: Define four arrays $W_{\text{bias}}, W_{\text{spike}}, V_{\text{cost}}, V_{\text{path}}$.
- 3: **for** each edge e in the graph **do**
- 4: Define $W_{\text{bias}}(e) = w_e((\bar{P}_0(t), \bar{H}_0(t))_{t=1}^T)$.
- 5: Define $W_{\text{spike}}(e)$ as in (9).
- 6: **end for**
- 7: Define the array $\text{Thresh} = W_{\text{spike}}$.
- 8: **for** $\alpha \in \text{Thresh}$ **do**
- 9: Solve the shortest-path problem from s to q for \mathcal{G}_α .
Let $\text{Path}_{s \rightarrow q}$ the optimal path. If there's a tie, favor the path with the lower maximal W_{spike} .
- 10: Define $V_{\text{path}}(\alpha) = \text{Path}_{s \rightarrow q}$.
- 11: Define $V_{\text{cost}}(\alpha) = \sum_{e \in \text{Path}_{s \rightarrow q}} W_{\text{bias}}(e) + \max_{e \in \text{Path}_{s \rightarrow q}} W_{\text{spike}}(e)$, the cost of the path $\text{Path}_{s \rightarrow q}$ for the problem (10).
- 12: **end for**
- 13: Find $\gamma = \arg \min_\beta V_{\text{cost}}(\beta)$.
- 14: **return:** $V_{\text{cost}}(\gamma), V_{\text{path}}(\gamma)$.

Proof. Let $\text{Path}_{s \rightarrow q}^*$ be the optimal solution of (RSPP). By optimality, for any other path $\text{Path}_{s \rightarrow q}$ at least one of the following holds:

$$\sum_{e \in \text{Path}_{s \rightarrow q}^*} W_{\text{bias}}(e) \leq \sum_{e \in \text{Path}_{s \rightarrow q}} W_{\text{bias}}(e), \quad (11)$$

$$\max_{e \in \text{Path}_{s \rightarrow q}^*} W_{\text{spike}}(e) \leq \max_{e \in \text{Path}_{s \rightarrow q}} W_{\text{spike}}(e), \quad (12)$$

where if at least one holds with equality, then both inequalities hold. Consider the graph \mathcal{G}_α for $\alpha = \max_{e \in \text{Path}^*} W_{\text{spike}}(e)$. For this graph, if a path $\text{Path}_{s \rightarrow q}$ satisfies the inequality (12), it does so with equality. Thus, it must satisfy (11), meaning that Path^* is the shortest path from s to q in \mathcal{G}_α . By the tie break rule and conditions (11), (12), we conclude that $V_{\text{path}}(\alpha) = \text{Path}^*$. Moreover, for any path $V_{\text{path}}(\beta)$, we have that:

$$V_{\text{cost}}(\beta) = \sum_{e \in V_{\text{path}}(\beta)} W_{\text{bias}}(e) + \max_{e \in V_{\text{path}}(\beta)} W_{\text{spike}}(e)$$

Thus, by optimality of Path^* , $\alpha = \arg \min_\beta V_{\text{cost}}(\beta)$, and the returned path is Path^* . This proves the correctness of the algorithm.

As for the time complexity, the parts outside the for-loop on α take $O(|\mathcal{E}|)$ time. Inside the for-loop, we build the graph \mathcal{G}_α , which takes $O(|\mathcal{E}|)$ time, and then solve the shortest-path problem on it, which also takes $O(|\mathcal{E}|)$ time, as it is a DAG. As the for-loop has $O(|\mathcal{E}|)$ iterations, we get a complexity of $O(|\mathcal{E}|^2)$ time. \square

Remark 2. *The complexity bound $O(|\mathcal{E}|^2)$ can sometimes be too high for real-world economic dispatch problems, in which the graph \mathcal{G} can have more than a million edges [12]. Instead, we note that if $\delta_{P,t}, \delta_{H,t}$ defined in (7) do not change too often,*

the array Thresh contains many repetitions. If Thresh contains $L \leq |\mathcal{E}|$ different elements, then the computational complexity of the algorithm is $O(|\mathcal{E}|L)$. We denote the number of different values that $\delta_{P,t}, \delta_{H,t}$ take for $t = 1, \dots, T$ as n_P, n_H respectively. It's easy to see that if $T \gg \max_{x,u} c(x, u)$, so each possible transition appears about the same number of times, then L scales linearly with $n_P + n_H$. Thus, we get that $L = O\left(\frac{|\mathcal{E}|}{T}(n_P + n_H)\right)$. Therefore, we get an algorithm whose time complexity $O(|\mathcal{E}|L) = O\left(\frac{|\mathcal{E}|^2}{T}(n_P + n_H)\right)$ grows linearly with the time horizon T , as for a fixed state-space representation, $|\mathcal{E}| = O(T)$ holds.

Algorithm 1, together with Remark 2, give a linear-time algorithm if most $\delta_{P,t}, \delta_{H,t}$ have the same value. If this is not the case, we can give a linear-time algorithm that achieves an approximation of the optimal solution. Namely, we prove the following:

Lemma 1. Consider the problem (RSPP) for the uncertainty set \mathcal{W} of the form (7), and let $\text{Path}_{s \rightarrow q}^*$ be the optimal solution. $\alpha = \max_{e \in \text{Path}^*} W_{\text{spike}}(e)$, and let $\beta \geq \alpha$ be any number. We let $\text{Path}_{s \rightarrow q}^\beta$ denote the shortest path from s to q in \mathcal{G}_β . We denote:

$$V^* = \sum_{e \in \text{Path}_{s \rightarrow q}^*} W_{\text{bias}}(e) + \max_{e \in \text{Path}_{s \rightarrow q}^*} W_{\text{spike}}(e)$$

$$V^\beta = \sum_{e \in \text{Path}_{s \rightarrow q}^\beta} W_{\text{bias}}(e) + \max_{e \in \text{Path}_{s \rightarrow q}^\beta} W_{\text{spike}}(e).$$

Then:

$$1) \text{ If } \epsilon = \beta - \alpha, \text{ then } V^* \leq V^\beta \leq V^* + \epsilon$$

$$2) \text{ If } \tau = \frac{\beta}{\alpha}, \text{ then } V^* \leq V^\beta \leq \tau V^*.$$

Proof. In both cases, it suffices to show that the right side of the inequality holds. First, as $\beta \geq \alpha$, the path $\text{Path}_{s \rightarrow q}^*$ has a finite cost in the graph \mathcal{G}_β , which is equal to its cost in \mathcal{G} . Thus, we conclude that

$$\sum_{e \in \text{Path}_{s \rightarrow q}^\beta} W_{\text{bias}}(e) \leq \sum_{e \in \text{Path}_{s \rightarrow q}^*} W_{\text{bias}}(e). \quad (13)$$

Moreover,

$$\max_{e \in \text{Path}_{s \rightarrow q}^\beta} W_{\text{spike}}(e) \leq \beta = \alpha + \epsilon \leq \max_{e \in \text{Path}_{s \rightarrow q}^*} W_{\text{spike}}(e) + \epsilon. \quad (14)$$

Summing (13) and (14) gives $V^\beta \leq V^* + \epsilon$. Moreover, as $\tau \geq 1$, we have,

$$\sum_{e \in \text{Path}_{s \rightarrow q}^\beta} W_{\text{bias}}(e) \leq \tau \sum_{e \in \text{Path}_{s \rightarrow q}^*} W_{\text{bias}}(e), \quad (15)$$

and

$$\max_{e \in \text{Path}_{s \rightarrow q}^\beta} W_{\text{spike}}(e) \leq \beta = \tau \alpha \leq \tau \max_{e \in \text{Path}_{s \rightarrow q}^*} W_{\text{spike}}(e). \quad (16)$$

Summing (15) and (16) gives $V^\beta \leq (1 + \mu)V^*$. \square

Lemma 1 can be used to prescribe linear-time algorithms approximating the optimal solution of (RSPP) for the uncertainty set (7):

Theorem 3. Consider Algorithm 1 and take any $\epsilon > 0$. Suppose that we change step 7 and define

$$\text{Thresh} = \left\{ \min_{e \in \mathcal{E}} W_{\text{spike}}(e), \min_{e \in \mathcal{E}} W_{\text{spike}}(e) + \epsilon, \right. \\ \left. \min_{e \in \mathcal{E}} W_{\text{spike}}(e) + 2\epsilon, \dots, \max_{e \in \mathcal{E}} W_{\text{spike}}(e) \right\}.$$

Let $V^{*,\epsilon}$ be the value provided by this modified algorithm, and let V^* be the optimal value of (RSPP) for the uncertainty set \mathcal{W} of the form (7). Then $V^* \leq V^{*,\epsilon} \leq V^* + \epsilon$. Moreover, the computational complexity of the modified algorithm is $O\left(|\mathcal{E}| \cdot \left\lceil \frac{\max_{e \in \mathcal{E}} W_{\text{spike}}(e) - \min_{e \in \mathcal{E}} W_{\text{spike}}(e)}{\epsilon} \right\rceil\right)$.

Proof. Suppose that α is $\max_e W_{\text{spike}}(e)$, where the maximum is taken over the optimal solution to (RSPP). By construction, there exists some $\beta \in \text{Thresh}$ such that $\beta \leq \alpha$ and $\epsilon \leq \beta - \alpha$. By Lemma 1, we conclude that $V^* \leq V_{\text{cost}}(\beta) \leq V^* + \epsilon$. By step 13, we have that $V^{*,\epsilon} \leq V_{\text{cost}}(\beta) \leq V^* + \epsilon$. The inequality $V^* \leq V^{*,\epsilon}$ is clear, as V^* is the optimal cost over all possible trajectories. Thus $V^* \leq V^{*,\epsilon} \leq V^* + \epsilon$. As for the time complexity, the same argument as in the proof of Theorem 2 shows that the time complexity is $O(|\mathcal{E}|N)$, where N is the number of points in Thresh. It can easily be seen that $N = \left\lceil \frac{\max_{e \in \mathcal{E}} W_{\text{spike}}(e) - \min_{e \in \mathcal{E}} W_{\text{spike}}(e)}{\epsilon} \right\rceil + 1$, which gives the desired complexity bound. This completes the proof. \square

Similarly, we prove:

Theorem 4. Consider Algorithm 1 and take any $\mu > 0$. Suppose that we change step 7 and define

$$\text{Thresh} = \left\{ \min_{e \in \mathcal{E}} W_{\text{spike}}(e), (1 + \mu) \min_{e \in \mathcal{E}} W_{\text{spike}}(e), \right. \\ \left. (1 + \mu)^2 \min_{e \in \mathcal{E}} W_{\text{spike}}(e), \dots, \max_{e \in \mathcal{E}} W_{\text{spike}}(e) \right\}.$$

Let $V^{*,\mu}$ be the value provided by this modified algorithm, and let V^* be the optimal value of (RSPP) for the uncertainty set \mathcal{W} of the form (7). Then $V^* \leq V^{*,\mu} \leq (1 + \mu)V^*$. Moreover, the computational complexity of the modified algorithm is $O\left(|\mathcal{E}| \cdot \left\lceil \frac{\log \max_{e \in \mathcal{E}} W_{\text{spike}}(e) - \log \min_{e \in \mathcal{E}} W_{\text{spike}}(e)}{\log(1 + \mu)} \right\rceil\right)$.

Proof. As before, let $\alpha = \max_e W_{\text{spike}}(e)$, where the maximum is taken over the optimal solution to (RSPP). By construction, there exists some $\beta \in \text{Thresh}$ such that $1 \leq \frac{\beta}{\alpha} \leq 1 + \mu$. By Lemma 1, we conclude that $V^* \leq V_{\text{cost}}(\beta) \leq (1 + \mu)V^*$. By step 13, we have that $V^{*,\mu} \leq V_{\text{cost}}(\beta) \leq (1 + \mu)V^*$. Together with $V^* \leq V^{*,\mu}$, stemming from optimality, we conclude that $V^* \leq V^{*,\mu} \leq (1 + \mu)V^*$. As for the time complexity, the same argument as in the proof of Theorem 2 shows that the time complexity is $O(|\mathcal{E}|N)$, where N is the number of points in Thresh. It can easily be seen that $N = \left\lceil \frac{\log \max_{e \in \mathcal{E}} W_{\text{spike}}(e) - \log \min_{e \in \mathcal{E}} W_{\text{spike}}(e)}{\log(1 + \mu)} \right\rceil + 1$, which gives the desired complexity bound. \square

C. Discussion about Uncertainty Sets

In the previous sections, we presented two possible choices for the uncertainty set. The first one, (6), can be understood as a norm ball of a weighed ℓ^∞ -norm, centred around the point $(P_0(t), H_0(t))$. Indeed, the condition in (6) can be restated as $\frac{1}{\Delta P(t)}|P(t) - P_0(t)| \leq 1$ and $\frac{1}{\Delta H(t)}|H(t) - H_0(t)| \leq 1$, which define a norm ball of radius 1 around the point $(P_0(t), H_0(t))$. The second choice of uncertainty set, (7), can be similarly seen as a Minkowski sum of two norm balls centred around $(P_0(t), H_0(t))$, the first being a weighted ℓ^1 -norm, and the second being a weighted ℓ^∞ -norm.

The tunable parameters $\Delta P(t), \Delta H(t), \delta_{P,t}, \delta_{H,t}, \mu_1$ are used to determine the size and exact shape of these uncertainty set. Figure 2 demonstrates the ℓ^1 -normed ball, ℓ^∞ -normed ball, and their Minkowski sum in \mathbb{R}^2 . It is seen in Figure 2 that with correct scaling, the Minkowski sum is a subset of an ℓ^∞ -normed ball which does not contain points in which all entries are “large” in absolute value, but still contains points in which a subset of the entries is large.

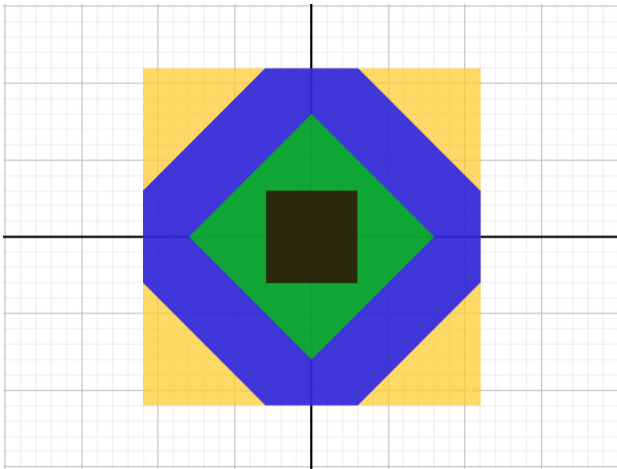


Fig. 2: Normed ball in \mathbb{R}^2 . The black set is an ℓ^∞ -normed ball, and the green set is an ℓ^1 -normed ball. The yellow set is a larger ℓ^∞ -normed ball, which is the analogue of (6). The blue set is the Minkowski sum of the black and purple sets, which is the analogue of (7). The blue set is a subset of the yellow set which does not include points in which both entries are large in absolute value.

Let us revert back to the uncertainty sets (6) and (7). With correct tuning, the set (7) is a subset of (6) which removes scenarios in which the realization of the demand uncertainty is “large” in absolute value for all times, but includes scenarios in which the realization of the demand uncertainty is “large” only for a subset of times. When solving (RSPP), smaller uncertainty sets allow us to reduce our conservatism, and hence improve our performance, assuming the uncertainty set contains the (unknown) true demand. This will become evident in the next section, which will test the prescribed algorithm in a case study.

IV. CASE STUDIES

A. Modeling and Pricing

We demonstrate the benefit of the presented algorithm in the economic dispatch of an MGT for CHP operation, whose cost functions are inspired by a discretized version of the Capstone C65 turbine [26]. The engine unit consists of a single stage centrifugal compressor, a can-type combustor, a single stage turbine, a recuperator and a separate heat recovery unit. In order to accommodate the changing ratio between power and heat generation demand, the recuperator is equipped with a controllable valve which alters the amount of exhaust gasses bypassing the heat exchanger. The schematic of the cycle is presented in Fig. 3.

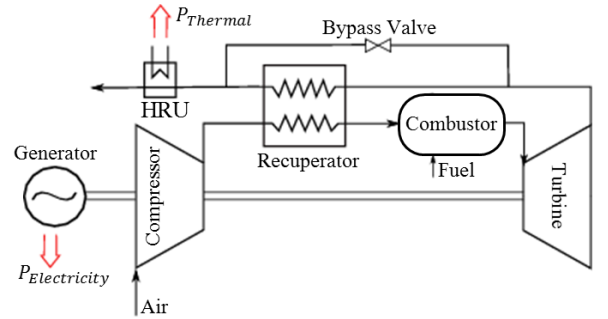


Fig. 3: Engine schematic cycle

In order to optimize the MGT cycle during its operation, two input parameters (shaft speed and recuperator bypass valve position) are selected and simulated to yield a number of solution states (electrical power and heat output that prescribes fuel mass flow). The discrete state space consists of 1501 states (1500 active states and one ‘off’ state), corresponding to 30 different engine shaft speeds (38.4 – 96 krpm) and 50 bypass valve positions (0 – 45%). The thermodynamic performance of the MGT is characterized in electrical power and heat output domains ranging between 5–65 kWel and 27–216 kW respectively; see Fig. 4(a)–(c). The lowest heat to power output ratio varies between 1.7–3.3 for 0–45% bypassing conditions.

We adopt the edge weight scheme appearing in [12] and determine the cost of an edge in the graph \mathcal{G} as follows: for an edge between a state $x(t_1)$ and a state $x(t_2)$, the power generation is defined as the average power $\frac{x(t_1) + x(t_2)}{2}$ times the transition time $t_2 - t_1$. The heat generation, fuel consumption and demand on the edge are defined similarly. The cost of the edge is now defined as the sum of the fuel cost, plus the cost of buying power and heat from the utility, while ensuring the power- and heat-balance equations are satisfied. In addition, there is a cost associated with the start-up and shut-down of the unit.

The cost of a gas turbine engine is roughly \$75,000. Thus, assuming a low cycle fatigue life of 10,000 cycles [60], we estimate the cost of shutdown and startup as \$3.75 each. During the start-up (lasting 6 minutes) and shut-down (lasting 3 minutes) sequences, we assume the MGT is offline for the entire duration, so all power and heat must be purchased from the utility.

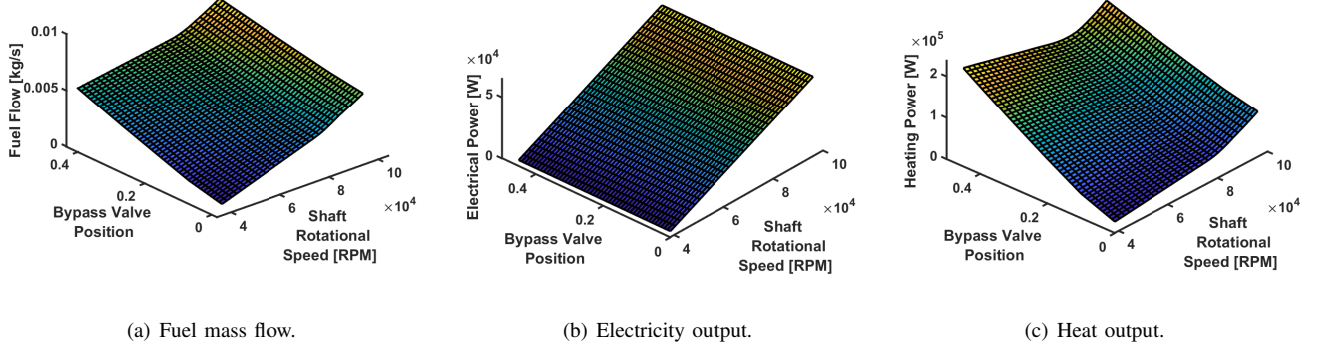


Fig. 4: Solution grid over the states of the gas turbine model.

The dispatch problem is considered for a residential building of multiple apartments. The demand profile of each apartment stems from the data published by the U.S. Department of Energy for the entire year of 2004 [61]–[63]. Within this database, we only consider the residential buildings internally specified as “Residential High.”³ In order to decide how many apartments benefit from the same MGT, the demand is scaled such that 95% of the time, the turbine’s electrical capacity is 80% of the consumer demand. This roughly corresponds to the needs of 9.3 apartments for our 65kWe turbine capacity.

For the cost of energy supplied from the utility, the price of electricity was determined according to data from PSEG Long Island New York [64], similar to [12]. In particular, the price of electricity is different between peak hours⁴ and off-peak hours, as well as between winter days⁵ and summer days.⁶ See [12, Table 2,3] for residential buildings for more information. In addition to electricity, the energy source for heat/chill can also be obtained from the utility to achieve energy balance between the demand and supply. As most consumers use a boiler to satisfy their heat demand, we model the heating cost with the price of natural gas - as shown in Eq. 24 in Ref. [12]. As for the cost of energy supplied by the MGT, the natural gas is the only consumable. The price of natural gas was taken to be \$18.42 per thousand cubic feet⁷, which was the residential price of natural gas in August 2020 [65]. If the MGT produces excess electricity beyond that of the local demand, the output is sold to the utility at the same tariff rate as the retail cost.

B. Algorithms and Running Time

We treat the year 2004 as real time for assessing the performance of each algorithm. The dispatch problem is considered for a horizon of 24 hours, dividing it to $T = 5760$ intervals, each 15 seconds long. Although we have the ground-truth demand for each day, it is not available when solving the economic dispatch problem in practice, since we can not predict the “future” accurately. Instead, we must use an

³The full name of the file is USA_NY_New.York-Central.Park.725033_TMY3_HIGH.csv

⁴These are the hours between 10AM and 8PM.

⁵These are days between October 1st and May 31st.

⁶These are days between June 1st and September 30th.

⁷Or equivalently, about 95 cents per kilogram.

estimate of the demand. For a given day, we use the ground-truth demand data from the previous two weeks (which are indeed available in practice while solving the ED problem) to compute an estimate of the demand for that day. For each time of day t , we compute the sample mean $\mu_P(t), \mu_H(t)$ and the standard deviation $\sigma_P(t), \sigma_H(t)$ of both power and heat demand from the preceding two weeks.

The performance of three algorithms are compared. Firstly, the ED algorithm from [12] that does not account for demand uncertainty is applied to the forecasted mean demand $(\mu_P(t), \mu_H(t))$ - we term this as the *nominal* algorithm. Moreover, the two robust ED algorithms presented in this work are considered. Their uncertainty sets use the standard deviation $\sigma_P(t), \sigma_H(t)$ of the power and heat demands, in addition to the forecasted mean demand.

The first uncertainty set we choose is of the form (6) with $P_0(t) = \mu_P(t), H_0(t) = \mu_H(t)$ and $\Delta P(t) = \alpha_{\mathcal{L}_\infty} \sigma_P(T), \Delta H(t) = \alpha_{\mathcal{L}_\infty} \sigma_H(t)$ for some parameter $\alpha_{\mathcal{L}_\infty} > 0$. The tuning parameter $\alpha_{\mathcal{L}_\infty}$ represents the trade-off between conservatism and accuracy. If $\alpha_{\mathcal{L}_\infty}$ grows larger, then the probability that the ground-truth demand is inside the uncertainty set becomes bigger. However, this also implies that the algorithm considers greater likelihood for outlier events associated with worst-case demand profiles; hence the solution becomes more conservative. In this study, $\alpha_{\mathcal{L}_\infty}$ is selected to be 0.13.

The second uncertainty set we choose is of the form (7) where $P_0(t) = \mu_P(t), H_0(t) = \mu_H(t), \Delta P(t) = \alpha_{\text{Mixed},1} \sigma_P(T), \Delta H(t) = \alpha_{\text{Mixed},1} \sigma_H(t), \delta_{P,t} = \frac{1}{\sigma_P(t)}, \delta_{H,t} = \frac{1}{\sigma_H(t)}$, and $\mu_1 = \alpha_{\text{Mixed},2}$. The parameters $\alpha_{\text{Mixed},1}, \alpha_{\text{Mixed},2}$ determine the size of the uncertainty set and are tunable. Here, we chose $\alpha_{\text{Mixed},1} = 0.03$ and $\alpha_{\text{Mixed},2} = 40$.

All the algorithms were computed on a Dell Latitude 7400 computer with an Intel Core i5-8365U processor. The nominal algorithm utilizes the shortest path formulation presented in [12]. For the first robust ED algorithm choice, Corollary 1 shows that a single application of the shortest path algorithm suffices as well. Both the nominal algorithm and the first robust algorithm use the same underlying combinatorial solution provided by the MATLAB internal shortest path solver, meaning they have nearly identical running times. For a total

of 1500 discretization level combinations, building the graph and finding the shortest path takes about 2 minutes. For the second robust ED algorithm choice, we must apply Algorithm 1. As the number of edges in the underlying graph is in the millions, the application of Algorithm 1 would require running the shortest path algorithm on roughly 10 million different graphs. We instead use the approximate version described in Theorem 3, where ϵ is chosen such that exactly $N = 30$ applications of the shortest path problems are performed. Even then, the runtime is significantly longer, about 7 minutes. However, it is still considered fast enough to be applicable in real-world systems. (Note that these runtimes can vary for different choices of the turbine discretizations.)

In addition to these three cases that forecast the demand, in order to contrast the performance of the algorithms with the global optimum, the shortest-path algorithm is applied to the ground-truth demand, which cannot be used in practice, as this quantity is unknown at the time of scheduling. Since this case produces the best possible schedule, we present it as the "benchmark" in all solutions.

C. Schedules and Associated Costs for Residential Buildings

In order to demonstrate the performance of the algorithms, a few exemplary days were analyzed considering their known two week demand histories: one winter day (February 5th), one spring day (March 24th), one summer day (June 28th), and one autumn day (September 19th). We note that the winter electricity tariff is used in the winter and spring days, whereas the summer electricity tariff is used in the summer and autumn days. For each day, the two robust algorithms (with demand uncertainty) and the nominal algorithm (without demand uncertainty) are evaluated based on the forecasted demand, and compared to the benchmark schedule stemming from known ground truth demand. Figures 5-8 present the resulting MGT electricity and heat production schedules of the 3 algorithms and contrasts it with the benchmark case utilizing ground-truth demand, which is also charted separately. The blue bands around the power and heat schedules indicate the forecasted demands with the standard deviations utilized in the uncertainty sets of the robust algorithms. In order to clarify the actual impact on the engine control parameters, spool speed and bypass valve position are separately charted for each algorithm. The schedules are computed for $T = 5760$ intervals, each 15 seconds long.

In the winter day of February 5th, Fig. 5, it can be seen that all four algorithms keep the MGT spool speed constant at its minimum operational value at almost all times, yielding the smallest amount of local electricity production, consistently below the power demand, which is predominantly met by purchase from the utility. However, the differences in schedules arise from changes in bypass valve schedule and the associated MGT heat production. The solution seems to be heat demand driven. The first robust algorithm gives the closest results to the benchmark case, followed by the second robust algorithm, and the worst case is the nominal algorithm absent of uncertainty.

Similarly, in the spring day of March 24th, Fig. 6, all four algorithms keep the MGT spool speed constant at its minimum

operational value at almost all times, significantly below the power demand, which is met by purchase from the utility. The second robust algorithm produces the same schedule as the nominal algorithm, but the first robust algorithm and the benchmark induce different schedules by choosing different trajectories for the bypass valve. The first robust algorithms slightly outperforms the others, although the schedules produced by all three algorithms have similar associated costs.

In the summer day of June 28th, Fig. 7, the first robust algorithm and the nominal algorithm produce identical schedules, and the second robust algorithm produces almost the same schedule as the benchmark. All algorithms decide to start the day operational. In the morning hours of the day (0-10AM), the MGT spool speed is near its minimum level and the electricity production is below the local demand. Moreover, the bypass valve is set to 0%. At around 10am, the MGT spool speed increases to about 78kRPM in order to satisfy the local demand. However, the electricity output of the turbine is not maximized, as the MGT does not reach its highest rpm. This appears to be an electricity demand driven operation, which lasts until around 19:00. From 20:00 until midnight, the first robust and the nominal algorithms decide to turn the turbine off, whereas the second robust algorithm decides to keep it operating close to the minimum capacity. In fact, the second robust algorithm achieves a nearly identical schedule to the benchmark, with only a small change around 8-9PM, and a difference in cost of less than 1 cent.

In the fall day of September 19th, Fig. 8, according to the benchmark case, the optimal schedule is to not turn on the MGT and keep it shut down the entire day. Only the second robust algorithm manages to replicate this behaviour. Both the first robust and the nominal algorithms turn on the turbine, and achieve an identical schedule, incurring an additional cost of about \$6.4.

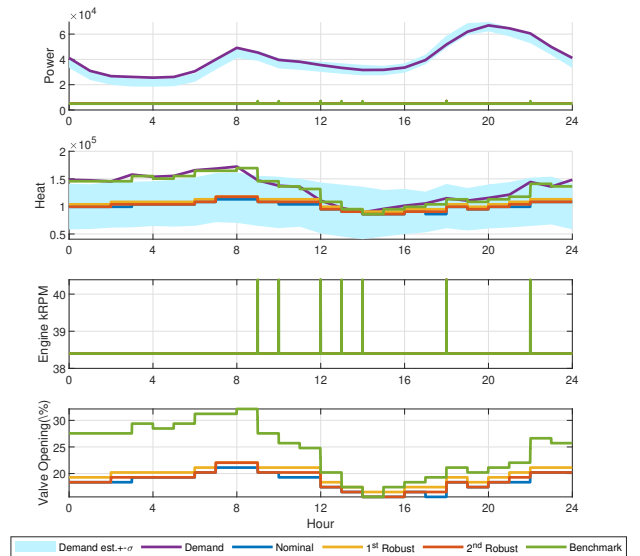


Fig. 5: The schedules produced by the algorithms for the winter day, February 5th. The horizontal axis represents the hour of day.

Table I summarizes the daily scheduling cost of all cases,

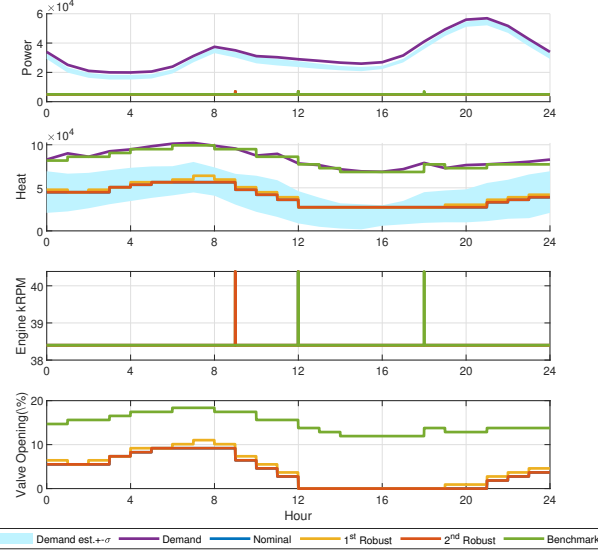


Fig. 6: The schedules produced by the algorithms for the spring day, March 24th. The horizontal axis represents the hour of day. The second robust algorithm produces the same schedule as the nominal algorithm.

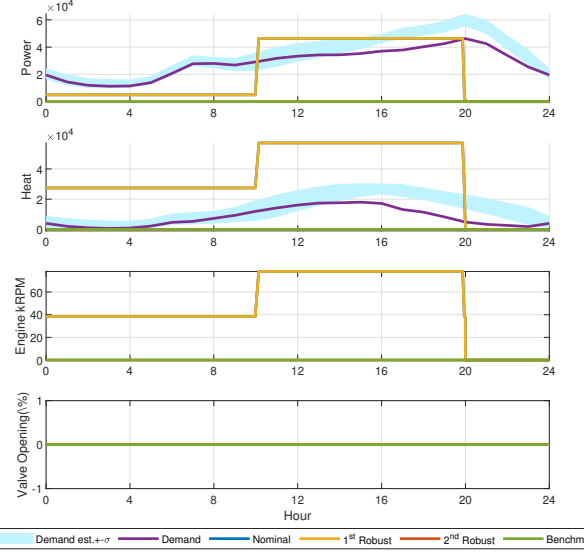


Fig. 8: The schedules produced by the algorithms for the autumn day, September 19th. The horizontal axis represents the hour of day. The first robust algorithm produces the same schedule as the nominal algorithm, and the second robust algorithm produces the same result as the benchmark.

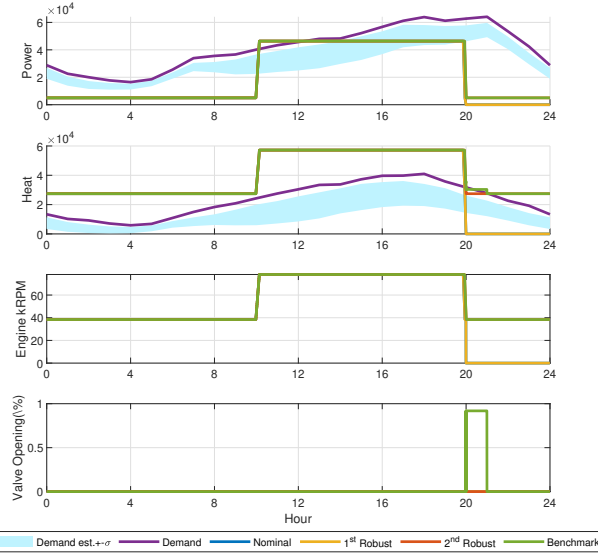


Fig. 7: The schedules produced by the algorithms for the summer day, June 28th. The horizontal axis represents the hour of day. The first robust algorithm produces the same schedule as the nominal algorithm, and the second robust algorithm produces a nearly identical schedule to the benchmark.

where the most favorable forecasting solution of that day is highlighted by italics. In each of the days, both robust algorithms perform at least as well as the nominal algorithm. Moreover, the first robust algorithm outperformed the nominal algorithm for all days with winter electricity tariff, with savings up to \$0.89 per day. The second robust algorithm outperformed the nominal algorithm for all days with summer electricity tariff, with savings up to \$6.37 per day. In fact, the second robust algorithm has exactly the same scheduling cost as the benchmark case in these days, meaning it successfully

finds the global minimum.

We can consider an alternative performance metric for the robust algorithms. It is clear that the benchmark cost is the optimum over all possible schedules. The nominal algorithm is an uncertainty-agnostic algorithm which represents the baseline from which we begin, in an effort to reduce the cost. The margin in cost between the nominal algorithm and the benchmark represents the potential benefit that any robust algorithm can offer. In table I, indicated in parentheses, we calculate the reduction of excess cost as a percentage of this margin, such that 100% and 0% reduction, implies that the robust algorithm performs identically to the benchmark and nominal cases respectively. For the four days considered, the first robust algorithm has an average reduction in excess cost of about 4%, and the second robust algorithm has an average reduction in excess cost of about 51%. This is expected considering the discussion in Section III-C that indicates that the first robust algorithm has an uncertainty set of the form (6) and the second robust algorithm has an uncertainty set of the form (7).

V. CONCLUSION

We considered the economic dispatch problem with forecasted demand for a single micro gas turbine, providing combined heat and power, coupled with utility. We assumed that the dynamics of the turbine are given by a discrete state-space model, which can be achieved by discretizing the operational regions of a gas turbine map, characterizing the fuel consumption as a function of spool speed and bypass valve position, that prescribes the local electricity and heat production. We considered the case in which the demand is unknown, but is rather assumed to be contained in a given uncertainty set. Two different models of an uncertainty set

Schedule Cost in \$ (Reduction in Excess Cost in %)	Winter Feb. 5 th	Spring Mar. 24 th	Summer Jun. 28 th	Autumn Sep. 19 th
Benchmark Case	293.02	196.86	188.83	126.48
Nominal Algorithm	299.39	202.30	191.35	133.32
First Robust Algorithm	<i>298.48</i> (14.29%)	<i>202.16</i> (2.57%)	<i>191.35</i> (0.00%)	<i>133.32</i> (0.00%)
Second Robust Algorithm	299.16 (3.61%)	202.30 (0.00%)	<i>188.83</i> (100.00%)	<i>126.48</i> (100.00%)

TABLE I: Schedule costs for the benchmark algorithm, the nominal algorithm, and the two robust algorithms. The reduction of excess costs for the robust algorithms compared to the nominal algorithm is displayed in parentheses. The costs associated with the best-performing algorithm in each day are highlighted by italics.

were proposed: one including time-dependent confidence intervals with no further assumption, and another coupling with a budgeting assumption throughout the time horizon. In the first case, we reduced the problem to a shortest path problem, resulting in a linear-time algorithm for finding the optimal solution. In the second case, we constructed an algorithm finding the optimal solution in quadratic time, and explained how to modify it to give an approximate optimal solution in linear time. Both algorithms were presented in a case study, in which we examined the performance of the proposed algorithms under realistic demand framework and tariffs of a residential unit. Under certain conditions, the findings indicate that mixed norm robust algorithm with forecasted demand and uncertainty sets reaches the globally optimal schedule stemming from a fully known heat and power demand.

This is a first step toward a robust integration of micro gas turbines with complex models and restrictions into a microgrid setting, which cannot deterministically predict the future demand. Future work can try to extend this framework for multiple turbines by using a dual-gradient algorithm, which will employ the robust algorithms described herein as intermediate steps when calculating the gradient.

VI. ACKNOWLEDGMENTS

The authors acknowledge the financial support of Minerva Research Center for Micro Turbine Powered Energy Systems (Max Planck Society Contract AZ5746940764), and Startups in Energy Program of Israeli Ministry of Energy (Contract 20180805). The first author thanks Dean Leitersdorf for helpful discussions.

REFERENCES

- [1] P. Criqui, “Prospective outlook on long-term energy systems,” 1996.
- [2] P. Capros, A. De Vita, L. Höglund Isaksson, W. Winiwarter, P. Purohit, H. Bottcher, S. Frank, P. Havlik, M. Gusti, and H. Witzke, *EU energy, transport and GHG emissions trends to 2050-Reference scenario 2013*. European Commission, 2013.
- [3] “U.S. Energy Information Administration.” Annual energy outlook 2015, <http://www.eia.gov/forecasts/aeo/> [Accessed: 2020-08-09].
- [4] P. Pilavachi, “Mini-and micro-gas turbines for combined heat and power,” *Applied thermal engineering*, vol. 22, no. 18, pp. 2003–2014, 2002.
- [5] J. Peirs, T. Waumans, P. Vleugels, F. Al-Bender, T. Stevens, T. Verstraete, S. Stevens, R. D’hulst, D. Verstraete, P. Fiorini, *et al.*, “Micropower generation with microturbines: a challenge,” *Proceedings of the Institution of Mechanical Engineers, Part C: Journal of Mechanical Engineering Science*, vol. 221, no. 4, pp. 489–500, 2007.
- [6] W. Gu, Z. Wu, R. Bo, W. Liu, G. Zhou, W. Chen, and Z. Wu, “Modeling, planning and optimal energy management of combined cooling, heating and power microgrid: A review,” *International Journal of Electrical Power & Energy Systems*, vol. 54, pp. 26–37, 2014.
- [7] M. Liu, Y. Shi, and F. Fang, “Combined cooling, heating and power systems: A survey,” *Renewable and Sustainable Energy Reviews*, vol. 35, pp. 1–22, 2014.
- [8] S. M. Camporeale, P. D. Ciliberti, B. Fortunato, M. Torresi, and A. M. Pantaleo, “Externally fired micro gas turbine and orc bottoming cycle: optimal biomass/natural gas chp configuration for residential energy demand,” in *Turbo Expo: Power for Land, Sea, and Air*, vol. 56673, p. V003T06A020, American Society of Mechanical Engineers, 2015.
- [9] A. C. Ferreira, M. L. Nunes, S. F. Teixeira, C. P. Leão, Â. M. Silva, J. C. Teixeira, and L. A. Martins, “An economic perspective on the optimisation of a small-scale cogeneration system for the portuguese scenario,” *Energy*, vol. 45, no. 1, pp. 436–444, 2012.
- [10] L. Mongibello, N. Bianco, M. Caliano, and G. Graditi, “Influence of heat dumping on the operation of residential micro-chp systems,” *Applied energy*, vol. 160, pp. 206–220, 2015.
- [11] A. Pantaleo, S. Camporeale, and N. Shah, “Thermo-economic assessment of externally fired micro-gas turbine fired by natural gas and biomass: Applications in italy,” *Energy Conversion and management*, vol. 75, pp. 202–213, 2013.
- [12] J. F. Rist, M. F. Dias, M. Palman, D. Zelazo, and B. Cukurel, “Economic dispatch of a single micro-gas turbine under chp operation,” *Applied energy*, vol. 200, pp. 1–18, 2017.
- [13] H. H. Happ, “Optimal power dispatch - a comprehensive survey,” *IEEE Transactions on Power Apparatus and Systems*, vol. 96, no. 3, pp. 841–854, 1977.
- [14] A. J. Wood, B. F. Wollenberg, and G. B. Sheblé, *Power generation, operation, and control*. John Wiley & Sons, 2013.
- [15] D. Bertsekas, G. Lauer, N. Sandell, and T. Posbergh, “Optimal short-term scheduling of large-scale power systems,” *IEEE Transactions on Automatic Control*, vol. 28, no. 1, pp. 1–11, 1983.
- [16] G. Binetti, A. Davoudi, F. L. Lewis, D. Naso, and B. Turchiano, “Distributed consensus-based economic dispatch with transmission losses,” *IEEE Transactions on Power Systems*, vol. 29, no. 4, pp. 1711–1720, 2014.
- [17] D. Zelazo, R. Dai, and M. Mesbahi, “An energy management system for off-grid power systems,” *Energy Systems*, vol. 3, no. 2, pp. 153–179, 2012.
- [18] F. Guo, C. Wen, J. Mao, and Y.-D. Song, “Distributed economic dispatch for smart grids with random wind power,” *IEEE Transactions on Smart Grid*, vol. 7, no. 3, pp. 1572–1583, 2015.
- [19] L. G. Papageorgiou and E. S. Fraga, “A mixed integer quadratic programming formulation for the economic dispatch of generators with prohibited operating zones,” *Electric power systems research*, vol. 77, no. 10, pp. 1292–1296, 2007.
- [20] P. Shamsi, H. Xie, A. Longe, and J. Joo, “Economic dispatch for an agent-based community microgrid,” *IEEE Transactions on Smart Grid*, vol. 7, pp. 2317–2324, Sep. 2016.
- [21] K. Hindi and M. Ab Ghani, “Dynamic economic dispatch for large scale power systems: a lagrangian relaxation approach,” *International Journal of Electrical Power & Energy Systems*, vol. 13, no. 1, pp. 51 – 56, 1991.
- [22] D. W. Ross and S. Kim, “Dynamic economic dispatch of generation,” *IEEE Transactions on Power Apparatus and Systems*, vol. PAS-99, no. 6, pp. 2060–2068, 1980.
- [23] V. L. H. Kanchev, F. Colas and B. Francois, “Emission reduction and economical optimization of an urban microgrid operation including dis-

patched pv-based active generators,” *IEEE Transactions on Sustainable Energy*, vol. 5, pp. 1397–1405, Oct. 2014.

[24] Z.-X. Liang and J. D. Glover, “A zoom feature for a dynamic programming solution to economic dispatch including transmission losses,” *IEEE Transactions on Power Systems*, vol. 7, no. 2, pp. 544–550, 1992.

[25] B. Saravanan, S. Das, S. Sikri, and D. Kothari, “A solution to the unit commitment problem — a review,” *Frontiers in Energy*, vol. 7, no. 2, pp. 223–236, 2013.

[26] “Technical and service manual. Capstone microturbine, model C65.” <https://www.capstoneturbine.com/> [Accessed 2020-08-08].

[27] “AMT NIKE manual and engine log.” <http://www.amtjets.com/Nike.php> [Accessed: 2020-08-08].

[28] O. Bendiksen, “Recent developments in flutter suppression techniques for turbomachinery rotors,” *Journal of Propulsion and Power*, vol. 4, no. 2, pp. 164–171, 1988.

[29] F. N. Lee and A. M. Breipohl, “Reserve constrained economic dispatch with prohibited operating zones,” *IEEE transactions on power systems*, vol. 8, no. 1, pp. 246–254, 1993.

[30] U. S. A. Federal Aviation Administration. Department of Transportation, “Rules and regulations.” Vol. 71, No. 188, Sept. 28, 2006, pp. 56864–56866. <https://www.govinfo.gov/content/pkg/FR-2006-09-28/pdf/FR-2006-09-28.pdf> [Accessed: 2020-08-08].

[31] T. H. Cormen, C. E. Leiserson, R. L. Rivest, and C. Stein, *Introduction to algorithms*. MIT press, 2009.

[32] G. Gross and F. D. Galiana, “Short-term load forecasting,” *Proceedings of the IEEE*, vol. 75, no. 12, pp. 1558–1573, 1987.

[33] D. Akay and M. Atak, “Grey prediction with rolling mechanism for electricity demand forecasting of turkey,” *Energy*, vol. 32, no. 9, pp. 1670 – 1675, 2007.

[34] C. Yu, P. Mirowski, and T. K. Ho, “A sparse coding approach to household electricity demand forecasting in smart grids,” *IEEE Transactions on Smart Grid*, vol. 8, no. 2, pp. 738–748, 2017.

[35] S. Mirasgedis, Y. Sarafidis, E. Georgopoulou, D. Lalas, M. Moschovitis, F. Karagiannis, and D. Papakonstantinou, “Models for mid-term electricity demand forecasting incorporating weather influences,” *Energy*, vol. 31, no. 2, pp. 208 – 227, 2006.

[36] A. Ben-Tal, L. El Ghaoui, and A. Nemirovski, *Robust optimization*, vol. 28. Princeton University Press, 2009.

[37] W. Elsayed, Y. Hegazy, F. Bendary, and M. El-Bages, “A review on accuracy issues related to solving the non-convex economic dispatch problem,” *Electric Power Systems Research*, vol. 141, pp. 325–332, 2016.

[38] J. Zhao, F. Wen, Y. Xue, Z. Dong, and J. Xin, “Power system stochastic economic dispatch considering uncertain outputs from plug-in electric vehicles and wind generators,” *Dianli Xitong Zidonghua(Automation of Electric Power Systems)*, vol. 34, no. 20, pp. 22–29, 2010.

[39] J. Hetzer, C. Y. David, and K. Bhattacharai, “An economic dispatch model incorporating wind power,” *IEEE Transactions on energy conversion*, vol. 23, no. 2, pp. 603–611, 2008.

[40] J. Dhillon, S. Parti, and D. Kothari, “Stochastic economic emission load dispatch,” *Electric Power Systems Research*, vol. 26, no. 3, pp. 179–186, 1993.

[41] A. Lorca and X. A. Sun, “Adaptive robust optimization with dynamic uncertainty sets for multi-period economic dispatch under significant wind,” *IEEE Transactions on Power Systems*, vol. 30, no. 4, pp. 1702–1713, 2014.

[42] H. Ming, L. Xie, M. C. Campi, S. Garatti, and P. Kumar, “Scenario-based economic dispatch with uncertain demand response,” *IEEE Transactions on Smart Grid*, vol. 10, no. 2, pp. 1858–1868, 2017.

[43] A. A. Thatte, X. A. Sun, and L. Xie, “Robust optimization based economic dispatch for managing system ramp requirement,” in *2014 47th Hawaii International Conference on System Sciences*, pp. 2344–2352, IEEE, 2014.

[44] X. Yang, Y. Zhang, H. He, S. Ren, and G. Weng, “Real-time demand side management for a microgrid considering uncertainties,” *IEEE Transactions on Smart Grid*, vol. 10, pp. 3401–3414, May 2019.

[45] C. Zhang, Y. Xu, Z. Y. Dong, and K. P. Wong, “Robust coordination of distributed generation and price-based demand response in microgrids,” *IEEE Transactions on Smart Grid*, vol. 9, no. 5, pp. 4236–4247, 2018.

[46] Y. F. Du, L. Jiang, Y. Li, and Q. Wu, “A robust optimization approach for demand side scheduling considering uncertainty of manually operated appliances,” *IEEE Transactions on Smart Grid*, vol. 9, no. 2, pp. 743–755, 2018.

[47] G. Yu and J. Yang, “On the robust shortest path problem,” *Computers & operations research*, vol. 25, no. 6, pp. 457–468, 1998.

[48] H. Yaman, O. E. Karaşan, and M. Ç. Pınar, “The robust spanning tree problem with interval data,” *Operations Research Letters*, vol. 29, no. 1, pp. 31 – 40, 2001.

[49] R. Montemanni and L. M. Gambardella, “An exact algorithm for the robust shortest path problem with interval data,” *Computers & Operations Research*, vol. 31, no. 10, pp. 1667–1680, 2004.

[50] D. Bertsimas and M. Sim, “Robust discrete optimization and network flows,” *Mathematical programming*, vol. 98, no. 1-3, pp. 49–71, 2003.

[51] V. Gabrel, C. Murat, and L. Wu, “New models for the robust shortest path problem: complexity, resolution and generalization,” *Annals of Operations Research*, vol. 207, no. 1, pp. 97–120, 2013.

[52] Y. Zhang, S. Song, Z. M. Shen, and C. Wu, “Robust shortest path problem with distributional uncertainty,” *IEEE Transactions on Intelligent Transportation Systems*, vol. 19, no. 4, pp. 1080–1090, 2018.

[53] J. Bondy and U. Murty, *Graph Theory with Applications*. Macmillan, 1977.

[54] R. T. Rockafellar, *Convex analysis*. No. 28, Princeton university press, 1970.

[55] D. Bertsimas and M. Sim, “The price of robustness,” *Operations research*, vol. 52, no. 1, pp. 35–53, 2004.

[56] A. Martin, J. C. Müller, and S. Pokutta, “Strict linear prices in non-convex european day-ahead electricity markets,” *Optimization Methods and Software*, vol. 29, no. 1, pp. 189–221, 2014.

[57] M. Van Vyve *et al.*, “Linear prices for non-convex electricity markets: models and algorithms,” tech. rep., 2011.

[58] D. A. Schiro, T. Zheng, F. Zhao, and E. Litvinov, “Convex hull pricing in electricity markets: Formulation, analysis, and implementation challenges,” *IEEE Transactions on Power Systems*, vol. 31, no. 5, pp. 4068–4075, 2016.

[59] M. Beaudin and H. Zareipour, “Home energy management systems: A review of modelling and complexity,” *Renewable and sustainable energy reviews*, vol. 45, pp. 318–335, 2015.

[60] S. Majumdar, “Low-cycle fatigue and creep analysis of gas turbine engine components,” *Journal of Aircraft*, vol. 12, no. 4, pp. 376–382, 1975.

[61] “Commercial reference buildings.” <http://energy.gov/eere/buildings/commercial-reference-buildings> [Accessed 2020-08-31].

[62] “Building characteristics for residential hourly load data: based on building America house simulation protocols.” http://en.openei.org/doe-opendata/dataset/eadfdbd10-67a2-4f64-a394-3176c7b686c1/resource/cd6704ba-3f53-4632-8d08-c9597842fde3/download/_buildingcharacteristicsforresidentialhourlyloaddata_.pdf [Accessed 2020-08-31].

[63] “Commercial and residential hourly load profiles for all TMY3 locations in the united states. Office of Energy Efficiency & Renewable Energy (EERE).” <https://openei.org/datasets/dataset/commercial-and-residential-hourly-load-profiles-for-all-tmy3-locations-in-the-united-states> [Accessed 2020-08-31].

[64] “Tariff for electric service residential. PSEG LINY; 2016.” https://www.psegliny.com/files.cfm/rates_resi.pdf.

[65] “U.S. natural gas prices. U.S. Energy Information Administration.” https://www.eia.gov/dnav/ng/ng_pri_sum_dcu_nus_m.html [Accessed 2020-08-31].